Control of CO2 Permeability Change in Different Rank Coals during Pressure Depletion: An Experimental Study

ARTICLE *in* ENERGY & FUELS · JANUARY 2014

Impact Factor: 2.79 · DOI: 10.1021/ef402285n

CITATIONS
5

READS
25

6 AUTHORS, INCLUDING:

Dameng Liu
China University of Geosciences (Beijing)
76 PUBLICATIONS **835** CITATIONS
SEE PROFILE

Yanbin Yao
China University of Geosciences (Beijing)
55 PUBLICATIONS **751** CITATIONS
SEE PROFILE

Yidong Cai
China University of Geosciences (Beijing)
30 PUBLICATIONS **211** CITATIONS
SEE PROFILE

Huang Saipeng
China University of Geosciences (Beijing)
1 PUBLICATION **5** CITATIONS
SEE PROFILE

energy&fuels

Article

pubs.acs.org/EF

Control of CO_2 Permeability Change in Different Rank Coals during Pressure Depletion: An Experimental Study

Junqian Li, Dameng Liu,* Yanbin Yao, Yidong Cai, Lulu Xu, and Saipeng Huang

Coal Reservoir Laboratory of National Engineering Research Center of Coalbed Methane (CBM) Development and Utilization, School of Energy Resources, China University of Geosciences, Beijing 100083, People's Republic of China

ABSTRACT: The gas permeability of different rank coals varies because of the summative effects of increasing effective stress, gas slippage, and coal matrix shrinkage during gas pressure depletion. In this paper, the natures of CO_2 permeability change were primarily investigated in a high-volatile A bituminous coal (core D2-2), a moderate volatile bituminous coal (core S1), and an anthracite coal (core P11-2-1). Under a 4.3 MPa confining stress condition, as the gas pressure declines, the CO_2 permeability of core D2-2 gradually decreases and then has a slight increase at mean gas pressures of less than approximately 0.8 MPa, the CO_2 permeability of core S1 initially decreases but subsequently increases above a mean gas pressure of approximately 1.3 MPa, and the CO_2 permeability of core P11-2-1 continuously increases, especially at mean gas pressures of less than approximately 1.8 MPa. These pressure-depletion observations on CO_2 permeability are considered to be the result of three effects: (a) increasing effective stress decreases CO_2 permeability; (b) increased gas slippage increases CO_2 permeability exponentially, becoming significant at mean gas pressures of less than approximately 0.8 MPa for the three cores; and (c) a positive effect on CO_2 permeability from matrix shrinkage occurs at mean pressures of less than approximately 1.3 and 1.8 MPa for cores S1 and P11-2-1, respectively, whereas the CO_2 permeability of core D2-2 is negatively affected by matrix shrinkage at all tested pressures. Additionally, it is found that the three effects on the CO_2 permeability depend upon the permeability of the coal and gas pressure.

1. INTRODUCTION

Coal is generally characterized as a dual-porosity medium made up of a coal matrix block and a natural fracture/cleat network. Abundant pores in the coal matrix act as the main storage space for coalbed methane (CBM), most of which is adsorbed to the coal. Each matrix block is separated by two sets of approximately orthogonal and subvertically oriented cleats, which serve as the primary pathway for fluid transport. Considering these features, the coal structure has been modeled using collections of sheets, matchsticks, and cubes,[1] and matchsticks have become the standard for coal permeability modeling.[2−7]

As a specially stored gas, the recovery of CBM is a complicated process involving the desorption, diffusion, and seepage of gas and the two-phase flow of the gas−liquid.[8] First, production of water leads to a reservoir pressure decline until a critical desorption pressure is reached, at which point, CBM begins to desorb. Near the production well, CBM depletion begins within the cleat system. Subsequently, adsorbed CBM within internal pores of the coal desorbs and diffuses through the matrix block to reach the cleats, where it flows to the well borehole.[9] Flow of CBM through the cleats is pressure-driven and can be described using Darcy's law, whereas through the matrix, the flow is assumed to be driven because of the concentration difference and is modeled by Fick's law of diffusion.[3,10]

During CBM production, the structure of pore fractures within coals is altered because of an increase of the effective stress on cleats induced by reservoir pressure drawdown and matrix shrinkage associated with gas desorption. This change in structure results in a change in coal permeability.[13,14] To date, it has been generally accepted that (a) coal permeability exponentially declines with an increase in the effective stress and (b) this decline is potentially offset by the permeability enhancement because of matrix shrinkage. Commonly, matrix swelling/shrinkage is accompanied by a volumetric strain in coals, which further impacts the permeability of the coal.[3−5,15−19] Research has shown that matrix shrinkage/swelling is closely related to the pressure and type of gas adsorbed and the rank of coals.[20,21] In a study by Day et al.,[22] the matrix swelling associated with carbon dioxide (CO_2) adsorption was expressed as a function of the gas density, which is a function of both the pressure and temperature of the gas. With respect to adsorbing gases, the adsorption capacity of CO_2 is greater than that of CBM because CO_2 not only adsorbs on the surface of coals but also partially dissolves in the matrix, modifying the physical structure of the coal matrix.[23−26]

To simulate the change of coal permeability, a number of analytical or coupled models have been developed by researchers.[2,4,6,7,13,27−32] The establishment of these models was based on different assumptions with respect to coal reservoir variation during the CBM recovery, such as uniaxial strain, constant volume, or constant confining stress. However, previous research usually assumed only effective stress and matrix shrinkage as the key factors influencing permeability change, neglecting the effect of gas slippage. As a significant factor influencing gas permeability, the gas slippage usually occurs in lowly permeable porous media and plays a positive role in the increase of gas permeability. Therefore, effective stress, matrix shrinkage, and gas slippage typically simultaneously affect gas permeability in coals.[33,34] Moreover, the three

Received: November 19, 2013
Revised: January 15, 2014
Published: January 15, 2014

   dx.doi.org/10.1021/ef402285n | *Energy Fuels* 2014, 28, 987−996

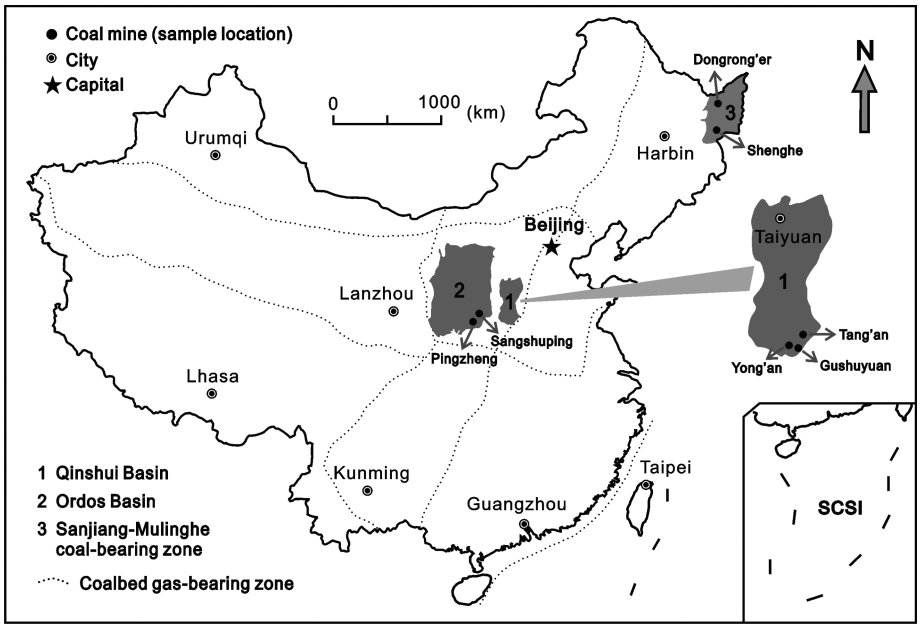

Figure 1. Location of the coal samples studied in this paper.

Table 1. Basic Information of Cores Used for the Permeability Test[a]

core number	coal mine	coal seam	L (cm)	R (cm)	D (g/cm^3)	$R_{o,max}$ (%)	V (%)	I (%)	E (%)	MM (%)
TA1-1	Tang'an	1	33.37	25.33	1.39					
Y3-2-1	Yong'an[b]	3	25.43	25.32	1.64	4.20	85.8	7.0	0.0	7.2
Y3-2-2			27.81	25.33	1.89	4.69	76.2	19.0	0.0	4.8
G15-3-1	Gushuyuan[b]	15	42.18	25.29	1.51					
G15-3-2			42.89	25.27	1.53	4.32	69.1	27.5	0.0	3.4
G15-3-3			27.39	25.25	1.49					
D2-2	Dongrong'er	2	34.04	25.34	1.34	0.84	66.0	3.6	29.8	0.6
S1	Shenghe	1	26.95	25.33	1.33	1.29	78.0	18.5	0.0	3.5
P11-2-1	Pingzheng[b]	11	23.67	25.34	1.38	2.79	69.3	21.7	0.0	9.0
P11-2-2			31.83	25.33	1.42					
S3-3-1	Sangshuping[b]	3	35.19	25.34	1.55	2.65[c]	72.3[c]	23.6[c]	0.0[c]	4.1[c]
S3-3-4			31.21	25.33	1.46					

[a] L, core length; R, core diameter; D, core density; $R_{o,max}$, maximum vitrinite reflectance; V, vitrinite content; I, inertinite content; E, exinite content; and MM, mineral matter content. [b] Several cores were cut from a coal sample. [c] Average value.

effects cause varied results in CO_2 permeability for coals with differences in mechanical properties, porosity, and permeability, among other factors. In this paper, CO_2 was selected as a representative fluid medium for investigating different rank coal permeabilities to adsorbing gases and the changes in permeability that occur during gas pressure depletion under a constant confining stress condition. Three factors affecting CO_2 permeability were discussed in detail: effective stress, matrix shrinkage, and gas slippage. Furthermore, the changes in permeability caused by each of these three effects were calculated independently to better understand the mechanisms controlling changes in permeability.

2. EXPERIMENTAL SECTION

An experimental program was undertaken using a total of seven coal samples from seven active mines located in the Ordos basin (Pingzheng and Sangshuping mines), Qinshui basin (Tang'an, Gushuyuan, and Yong'an mines), and Sanjiang-Mulinghe coal-bearing zone (Dongrong'er and Shenghe mines) of China (Figure 1). All samples were wrapped in a timely manner with preservative films and were carefully transferred to the laboratory for experimental measurements. Then, the permeability tests were conducted on 12 columned cores cut perpendicular to the bedding surface at the Rock Mechanics Laboratory of China University of Petroleum (Beijing, China). Some essential information for these cores is presented in Table 1. Core preparation, permeability test procedure, and experimental setup have been detailed in the study by Li et al.[34] For several experimental instruments, including graduated cylinder, pressure gage, micrometer, and strain gages, their precisions are 0.2 mL, 0.001 × 0.1 MPa, 0.01 cm, and 0.001 mm, respectively. After the permeability test, the coal cores were further measured for maximum vitrinite reflectance and maceral compositions using a Leitz MPV-3 microscope by the Chinese Standard of GB/T 6948-1998 and GB/T 8899-1998, respectively.[35−37]

The objective of this experimental work was to investigate the mechanisms controlling changes in adsorbing gas (CO_2) permeability in different rank coals under a constant confining stress condition. If the confining stress acting on the coal is constant during the gas drainage, it follows that changes in coal reservoir conditions include only a decrease in the gas pressure and a corresponding increase in the effective stress. To simulate this process, a series of experimental conditions composed primarily of five effective stresses were first designed, as shown in Figure 2. Both the confining stress and the gas pressure were increased to keep a constant positive effective stress on the core under each effective stress condition. The stress and gas pressures applied to each core are illustrated in Figure 3. Next, gas

dx.doi.org/10.1021/ef402285n | Energy Fuels 2014, 28, 987−996

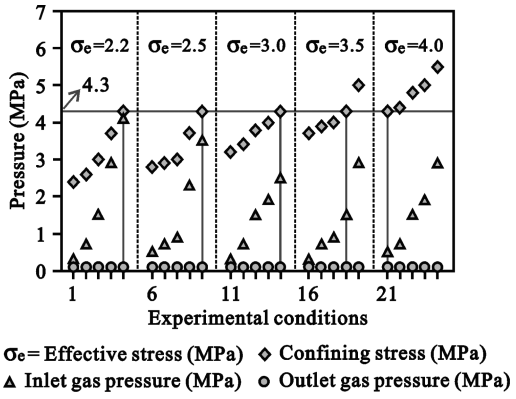

Figure 2. Experimental conditions for gas permeability tests.

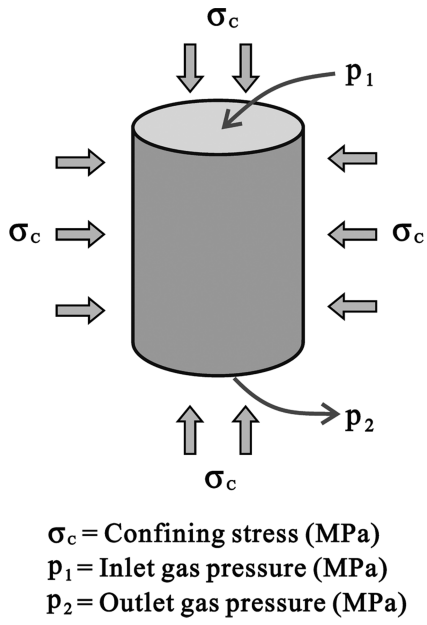

Figure 3. Schematic map of the stress and gas pressure applied to the core.

seepage behaviors with respect to CO_2 and helium (He) were analyzed to quantify increases in CO_2 permeability caused by gas slippage and matrix shrinkage at each experimental gas pressure under constant effective stress conditions. During this process, several crucial parameters, including the CO_2 gas slippage factor and the equivalent liquid permeability, were obtained following methods outlined in a previous study.[3] Finally, a set of CO_2 permeability data selected under a 4.3 MPa confining stress condition was used for achieving the goals of this study.

It should be noted that (a) the permeability test was performed first on He and then on CO_2 and (b) for each core, stress was applied in an increasing sequence to reduce the damage to cores from the adjustments in confining stress. In addition, the real-time strain in the core was monitored using a strain gauge.[34] The measured data were captured by a data acquisition system and, subsequently, outputted by a computer.

3. RESULTS AND DISCUSSION

3.1. Permeability Change. Test results for three typical cores are detailed in this paper. These three cores (D2-2, S1, and P11-2-1) have different metamorphic grades, varying from high-volatile A bituminous to anthracite rank, with a maximum vitrinite reflectance of 0.84, 1.29, and 2.79%, respectively. Permeability test results showed that core S1 had the highest permeability and core D2-2 had the lowest permeability for the same experimental conditions (inlet gas pressures of 0.3−4.1 MPa and confining stresses of 2.4−5.5 MPa; Figure 4). In

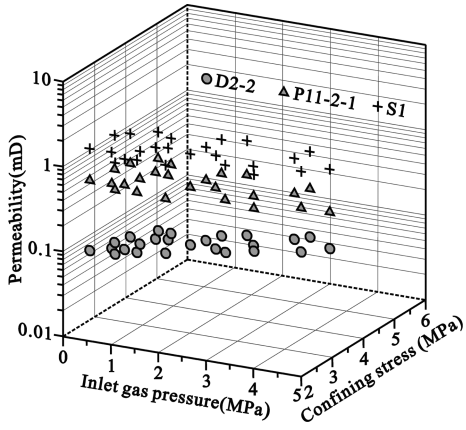

Figure 4. CO_2 permeabilities under inlet gas pressures of 0.3−4.1 MPa and confining stresses of 2.4−5.5 MPa conditions.

general, the permeability values ranged from 0.045 to 0.089 mD (averaging 0.066 mD), from 0.455 to 1.402 mD (averaging 0.794 mD), and from 0.174 to 0.619 mD (averaging 0.354 mD) for cores D2-2, S1, and P11-2-1, respectively (Figure 4). The differences in permeability may be closely related to naturally fractured networks within the coals, which act as the dominant pathway for free fluids.[38] In particular, the permeability for coals with well-developed open fractures will be high.[37]

Under a constant confining stress (4.3 MPa) condition, the changes in permeability of each of the three cores during the pressure depletion process were distinct. As the pressure declined from 4.1 to 0.5 MPa, the permeability of core D2-2 gradually decreased and then had a slight increase at inlet gas pressures of less than approximately 1.5 MPa (corresponding to mean gas pressures of less than 0.8 MPa), the permeability of core P11-2-1 increased especially at inlet gas pressures of less than 3.5 MPa (corresponding to mean gas pressures of less than 1.8 MPa), and the permeability of core S1 initially decreased before subsequently increasing at an inlet gas pressure of approximately 2.5 MPa (corresponding to a mean gas pressure of approximately 1.3 MPa; Figure 5). Additionally, the magnitude of CO_2 permeability variation was positively correlated to coal permeability. At different gas pressures, the permeability variation of core S1 ranged from 0 to approximately 0.332 mD, core D2-2 showed the least variation in CO_2 permeability, ranging from 0 to 0.024 mD, and core P11-2-1 ranged in CO_2 permeability from 0 to 0.214 mD.

3.2. Effect of Effective Stress on Permeability. Experimental measurements and even theoretical derivation have confirmed that coal permeability can be described as an exponential function of the effective stress.[2,39,40] Typically, the increase in effective stress resulted in the closure of the cleat/fracture of coals, which is one of the most significant factors influencing coal permeability loss during a pressure decline. The sensitivity of permeability to increases in effective stress was quantitatively represented by coal cleat compressibility. The cleat compressibility is defined as the ratio of cleat porosity variation per unit change in pressure to total cleat porosity and can be simply estimated according to the permeability-effective stress relationship

dx.doi.org/10.1021/ef402285n | Energy Fuels 2014, 28, 987−996

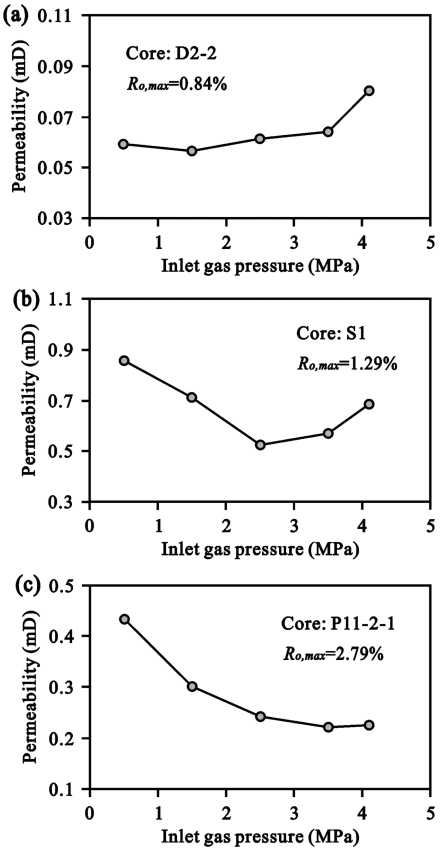

Figure 5. CO_2 permeability changes under a 4.3 MPa confining stress condition.

$$\ln \frac{k}{k_o} = -3c_f(\sigma - \sigma_o) \tag{1}$$

where k is the permeability (mD), σ is the effective stress (MPa), c_f is the coal cleat compressibility (MPa^{-1}), and the subscript "o" indicates initial conditions.

Thus, through fitting eq 1 to permeability-effective stress data, $-3c_f$ can be obtained as the slope of the straight line and is written as

$$-3c_f = \frac{\ln \frac{k}{k_o}}{(\sigma - \sigma_o)} \tag{2}$$

Previous research has shown that coal cleat compressibility measured by gas is not a constant factor and is closely dependent upon the gas type, gas pressure, and temperature, among other factors.[41,42] In a study by McKee et al.,[27] coal cleat compressibility was theoretically assumed to decrease exponentially with increasing effective stress. Palmer[31] reported that under high-stress conditions, the cleat compressibility is reduced because of the stiffening of the constrained modulus (M) as porosity and permeability decrease. In this study, it can be seen that the cleat compressibilities measured by CO_2 not only varied for different cores but also varied with different gas pressures for the same core (Figure 6). The cleat compressibilities at inlet gas pressures of 0.7−2.9 MPa were maximal in core D2-2 (ranging from 0.0719 to 0.1003 MPa^{-1}), and were minimal in core S1 (0.044−0.0604 MPa^{-1}), approximating those of core P11-2-1 (0.0454−0.0739 MPa^{-1}). Thus, the strongest negative effect of the effective stress on the permeability occurred in core D2-2, and the relatively less negative effect occurred in cores S1 and P11-2-1. This result implies that the coal with a lower permeability will have a stronger sensitivity of the permeability to the effective stress. In addition, the cleat compressibility varies as gas pressure decreases, and the variation tendencies are different for the three cores. During the pressure decline, the cleat compressibility of core D2-2 gradually decreases; for cores S1 and P11-2-1, it initially decreases but subsequently increases slightly.

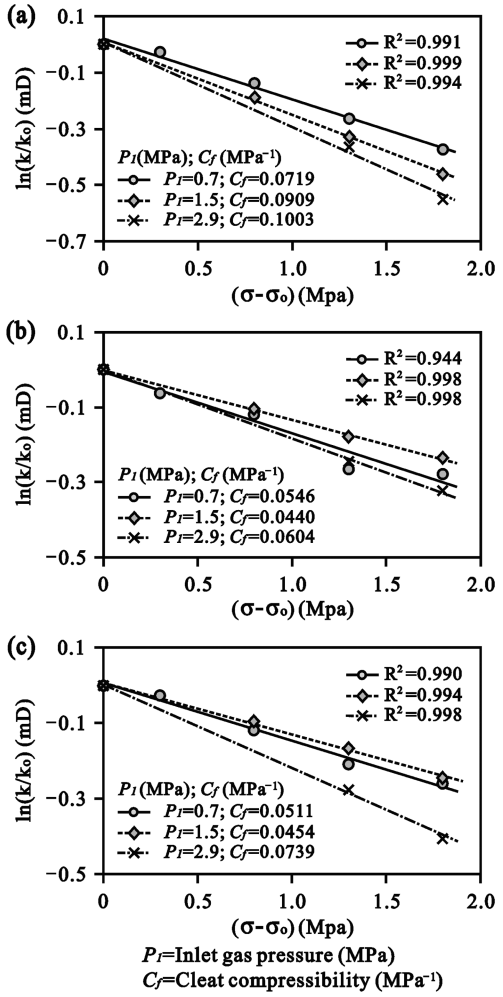

Figure 6. Coal cleat compressibilities measured by CO_2 at inlet gas pressures of 0.7, 1.5, and 2.9 MPa (a, core D2-2; b, core S1; and c, core P11-2-1).

In this study, a linear function was used to fit the permeability-effective stress data[12] to simply describe the impact of effective stress on permeability. As shown in Figure 7, it can be seen that the variations in the gradients of permeability (i.e., the slope of the straight line) are approximately equal at different gas pressures. On the basis of this observation, the accumulated permeability loss caused by the effective stress increase can be calculated and is given as a function of the average slope $\overline{k}$[34]

$$\Delta k_{eff}(p_t) = \overline{k}(p_i - p_t)/2 \tag{3}$$

where p_i indicates the initial inlet gas pressure, p_t is the instantaneous inlet gas pressure, and $\Delta k_{eff}(p_t)$ is the permeability loss associated with the effective stress increase as the inlet gas pressure is reduced from p_i to p_t.

dx.doi.org/10.1021/ef402285n | Energy Fuels 2014, 28, 987−996

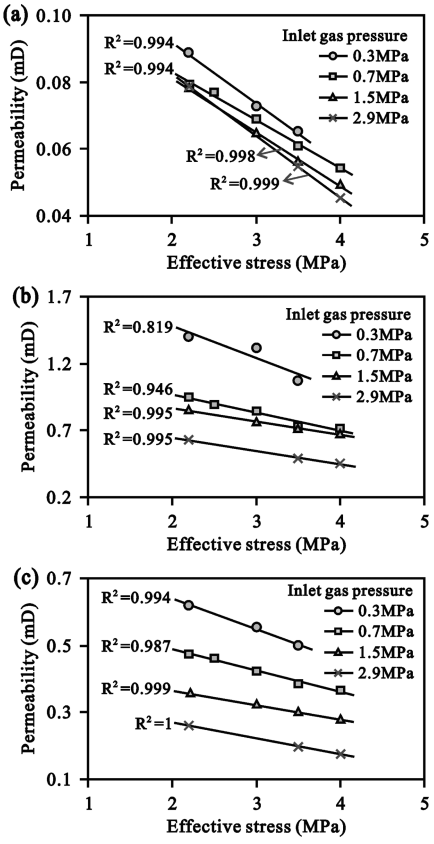

Figure 7. Relationships between CO_2 permeability and the effective stress (a, core D2-2; b, core S1; and c, core P11-2-1).

According to eq 3, it can be seen that the average slope $\overline{k}$ is a significant coefficient reflecting the permeability loss as the effective stress increases. Using the same unit system for the permeability and the effective stress, the average slopes are of −0.0168, −0.1434, and −0.0617 for cores D2-2, S1, and P11-2-1, respectively. This indicates that the permeability loss is the greatest for core S1 and a minimal loss occurs in core D2-2 for the same change in effective stress. It is thus clear that less permeable coals with higher stress sensitivity will have less permeability loss.

3.3. Effect of Gas Slippage on Permeability. The flow of fluids through minimally permeable porous media disobeys Darcy's law, leading to a difference between gas and liquid permeabilities. This difference is usually explained by taking gas slippage into account. Research[43] has shown that the gas slippage phenomenon depends upon the nature of gas and porous media and is thus associated with the mean free path of gas molecules and the mean radius of pores within porous media. Commonly, a linear relationship between gas permeability and the reciprocal of the mean gas pressure is considered to be a symbol of the gas slippage phenomenon. It is mathematically described[43] as

$$k_g = k_o\left(1 + \frac{b}{P_m}\right) \tag{4}$$

where k_g is the gas permeability, P_m is the mean gas pressure, k_o is a Klinkenberg-corrected value of k_g at an infinite mean gas pressure (also known as the equivalent liquid permeability), and b is the gas slippage factor.

Both the flows of He and CO_2 within the cores studied appear as the gas slippage phenomena at experimental gas pressures under the five effective stress conditions. On the basis of the slippage behavior of He, several parameters, including the equivalent liquid permeability and the He gas slippage factor, were obtained directly by fitting eq 4 to the experimental data under each effective stress condition. The CO_2 slippage factor was then calculated as a function of the He slippage factor. Further, the CO_2 permeability increments induced by the gas slippage and the matrix shrinkage were simultaneously obtained at each gas pressure.[34] Significant data are listed in Table 2.

Results showed that, under a 4.3 MPa confining stress condition, the permeability increments caused by the gas slippage and the matrix shrinkage can be mathematically expressed as a function of the difference between inlet and outlet gas pressures (Figure 8). The positive correlation between gas slippage and permeability can be expressed exponentially and usually becomes more significant at inlet gas pressures of less than 1.5 MPa. The gas slippage-induced permeability increment ($\Delta k_{sli}(p_t)$) at an inlet gas pressure of p_t can be written as

$$\Delta k_{sli}(p_t) = a_1(p_t - p_2)^{b_1} \tag{5}$$

where p_2 is the outlet gas pressure equal to the atmospheric pressure and a_1 and b_1 are dimensionless coefficients.

In addition to the gas pressure, the permeability of coal is another factor influencing the gas-slippage-dependent CO_2 permeability increment. As shown in Figure 9a, the CO_2 permeability increment was positively proportional to the permeability of coal. However, the CO_2 permeability increment values were low overall and varied from 0.008 to 165.374 μD as the gas pressure decreased from 4.1 to 0.5 MPa under a 4.3 MPa confining stress condition (Table 2).

3.4. Effect of Matrix Shrinkage on Permeability. Matrix shrinkage has a complex and variable effect on coal permeability. Through a correlation analysis, the matrix-shrinkage-induced permeability increments were found to change quadratically at different rates for each of the three cores (Figure 8). With the pressure decline, the permeability increment gradually decreased for core D2-2, while for cores S1 and P11-2-1, it initially decreased but subsequently increased. The most dramatic difference between the latter two cores is that, during the pressure depletion, the pressure at which the permeability increment began to increase was lower for core S1 (inlet gas pressure is of approximately 2.5 MPa) than that for core P11-2-1 (approximately 3.5 MPa). As shown in Figure 9b, at approximately 2.5 and 3.5 MPa inlet gas pressures, the permeability increments caused by the matrix shrinkage were relatively low for the coals with permeabilities greater than 0.1 mD. For the coals with a permeability of less than 0.1 mD, the permeability increments are high and level off to an approximately constant value. In general, the permeability increment gradually decreases in the form of a parabolic curve with the increase in coal permeability.

Two significant phenomena were noted: (a) a decrease stage occurred in the curve of the permeability increment caused by the matrix shrinkage, and (b) the decrease stage was longer for a lower rank coal. These might be the result of the difference in the adsorption capacity of CO_2 on different rank coals. Usually, as the rank of coal increases, swelling effects associated with adsorption go up.[20] Thus, the positive impact of the matrix shrinkage of coal will increase with an increasing metamorphic

dx.doi.org/10.1021/ef402285n | Energy Fuels 2014, 28, 987−996

Table 2. CO_2 Permeability Increments Caused by the Gas Slippage and the Matrix Shrinkage at Different Gas Pressures under a 4.3 MPa Confining Stress Condition[a]

	p_1 = 4.1 MPa			p_1 = 3.5 MPa			p_1 = 2.5 MPa			p_1 = 1.5 MPa			p_1 = 0.5 MPa		
core number	k_g	Δk_{sli}	Δk_{shr}	k_g	Δk_{sli}	Δk_{shr}	k_g	Δk_{sli}	Δk_{shr}	k_g	Δk_{sli}	Δk_{shr}	k_g	Δk_{sli}	Δk_{shr}
TA1-1	5.026	0.591	0.635	4.616	0.340	−1.824	2.449	0.614	−1.466	2.754	0.913	−0.659	5.030	1.527	−0.497
Y3-2-1	4.985	0.421	−6.536	4.758	0.255	−7.097	4.719	0.693	−2.674	4.811	0.913	−2.502	7.822	1.357	−1.435
Y3-2-2	15.452	0.842	−6.690	13.612	0.576	−8.164	11.327	1.268	−2.241	11.621	1.401	−5.081	16.646	3.563	−1.517
G15-3-1	0.070	0.016	−0.446	0.091	0.019	−0.328	0.091	0.013	−0.263	0.091	0.021	−0.207	0.091	0.057	0.124
G15-3-2	0.097	0.016	−0.219	0.111	0.019	−0.108	0.200	0.026	−0.126	0.293	0.021	−0.029	0.457	0.113	0.144
G15-3-3	0.114	0.008	−0.194	0.125	0.006	−0.180	0.186	0.013	−0.027	0.168	0.013	−0.145	0.343	0.045	0.097
D2-2	80.197	5.026	24.671	63.916	5.665	31.651	61.247	6.145	−5.098	56.259	8.838	0.121	58.919	16.203	−23.684
S1	683.774	33.847	−556.573	569.741	35.938	−547.497	523.391	43.563	−694.672	711.468	64.905	−452.336	855.293	165.374	−342.981
P11-2-1	224.502	21.100	−180.498	220.227	16.562	−247.435	242.062	26.344	−200.182	300.926	40.770	−91.644	433.863	68.608	−59.745
P11-2-2	186.198	21.472	8.026				192.665	19.749	−60.884	223.507	39.134	−57.227	306.971	77.503	−71.232
S3-3-1	4.111	0.291	−1.881	3.437	0.104	−6.067	2.744	0.301	−4.956	2.844	0.234	−6.290	5.824	0.737	−2.813
S3-3-4	3.216	0.202	2.514	2.560	0.142	1.118	2.144	0.170	−0.226	1.770	0.212	−0.543	2.413	0.340	−0.727

[a] p_1, inlet gas pressure; k_g, coal permeability to CO_2; Δk_{sli}, gas-slippage-induced permeability increment; and Δk_{shr}, matrix-shrinkage-induced permeability increment.

Figure 8. CO_2 permeability increments induced by the gas slippage and the matrix shrinkage under a 4.3 MPa confining stress condition (a, core D2-2; b, core S1; and c, core P11-2-1).

grade of coal. In comparison to coals studied in this paper, the increases in the permeability increment for anthracite coals are much more obvious on a linear or logarithmic scale.[34] Overall, the matrix-shrinkage-induced permeability increment $[\Delta k_{sli}(p_t)]$ for the three cores in this study can be written as

$$\Delta k_{shr}(p_t) = a_2(p_t - p_2)^2 + b_2(p_t - p_2) + c \quad (6)$$

where a_2, b_2, and c are dimensionless coefficients.

The matrix-shrinkage-induced permeability increment ranges from −694.672 to 31.651 μD (Table 2) and has a higher absolute value than the permeability increments caused by the gas slippage at the same experimental conditions. In Figure 9c, it also can be seen that the former is predominant in the total permeability increment caused by the two factors.

3.5. Strain Characteristics of Coals. During the gas pressure depletion, both the change in the stress acting on coals and the coal matrix shrinkage contribute to the structural deformation of coals, which follow the strain. Commonly, with respect to different rank coals, their strain characteristics associated with gas sorption/desorption or stress variation are diverse.[21,44] In this study, under the same gas pressure and confining stress conditions, core S1 showed the maximum

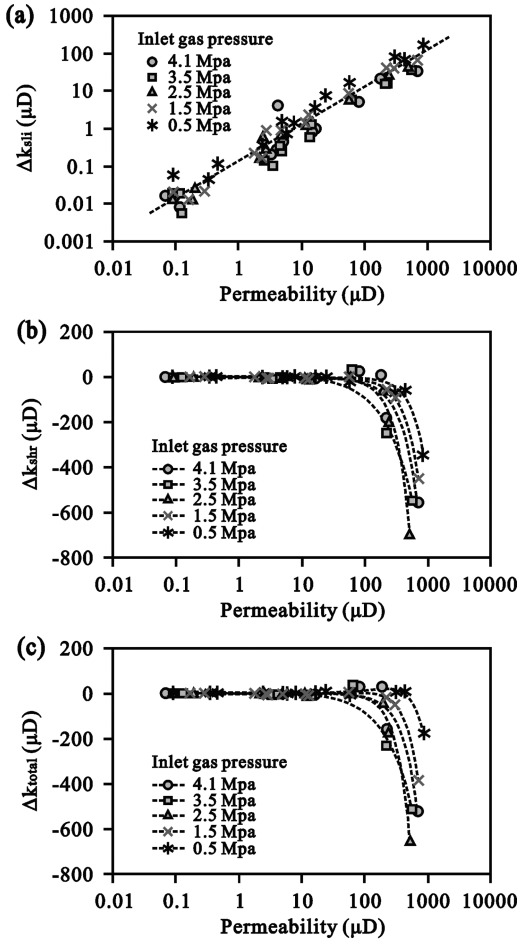

Figure 9. Relationships of coal permeability with CO_2 permeability increments induced by (a) gas slippage, (b) matrix shrinkage, and (c) these two factors.

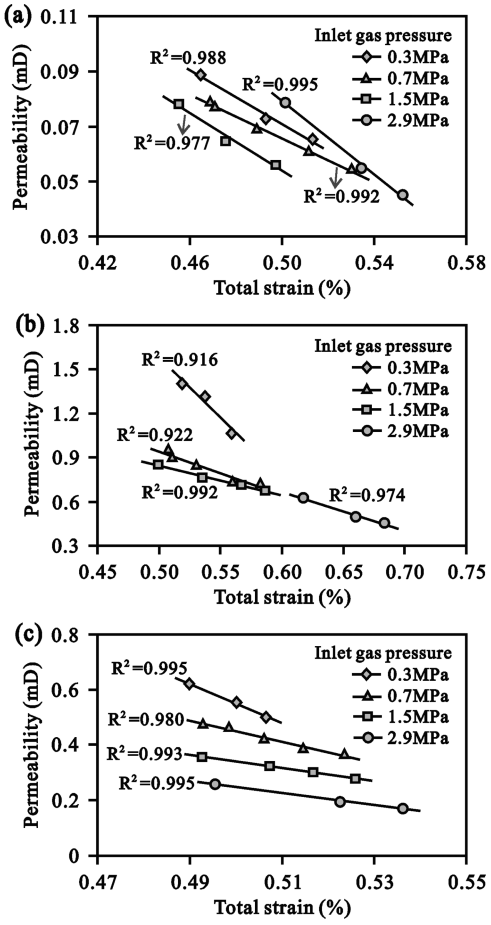

Figure 10. Relationship between CO_2 permeability and total strain for (a) core D2-2, (b) core S1, and (c) core P11-2-1.

strain compared to cores D2-2 and P11-2-1, of which core D2-2 showed the least strain and approximates that of core P11-2-1. This could be because the high permeability coal develops an open pore-fracture system, which tends to undergo great deformation under a certain stress. As the gas pressure declined, although the gas permeability variation tendencies were diverse for the three cores, a negatively linear relationship between the permeability and the total strain of coals measured at constant gas pressures for eliminating the impact of the gas slippage could be uniformly obtained (Figure 10). This result was consistent with the experimental research by Harpalani and Chen.[3]

Usually, the volumetric strain induced by sorption/desorption was described as a function of the gas pressure following a Langmuir-like equation.[15] In this paper, total strain depends upon the gas pressure and the effective stress. A gas-pressure-dependent strain reflects the impact of the matrix shrinkage on the coal structure and plays a significant role in offsetting the coal strain caused by the effective stress increase. As shown in Figure 11, under constant effective stress conditions, the strain induced by the gas pressure decrease was presented in a different manner for the three cores, of which the strain of core P11-2-1 continuously decreased, but cores S1 and D2-2 underwent a strain rebound, starting at the inlet gas pressure of 1.5 MPa. According to the gas pressure−strain relationships of the three cores, it is further suggested that the positive effect of the matrix shrinkage on the permeability increases with the increase in the coal metamorphic grade, as mentioned in section 3.4. In contrast, the effective stress increase is an important factor, causing the increase in the total strain of coals. The results showed that, with the increase in the effective stress, the total strain at the same gas pressures (i.e., the strain caused by the effective stress increase) linearly increased (Figure 12), which corresponds to a negative linear relationship between the permeability and the effective stress. It is thus considered that the essence of the coal permeability variation associated with the effective stress increase and the matrix shrinkage is due to the occurrence of strain in coals.

3.6. Mechanism of Permeability Change. Mathematical expressions representative of the effects of the effective stress, the gas slippage, and the matrix shrinkage on the permeability were presented in Table 3. On the basis of these expressions, a total permeability increment was obtained as an algebraic sum of the three individual permeability increments. As shown in Figure 13, the ideal change tendency of total permeability increments is consistent with the permeability change for the three cores. Furthermore, its numerical value is much greater for a higher permeability coal.

dx.doi.org/10.1021/ef402285n | Energy Fuels 2014, 28, 987−996

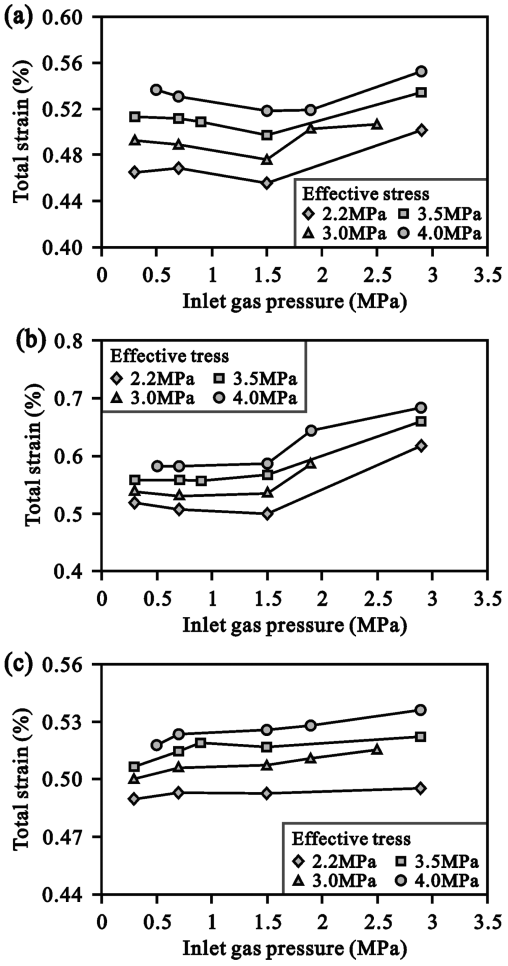

Figure 11. Relationship between the inlet gas pressure and the total strain of coal under constant effective stress conditions (a, core D2-2; b, core S1; and c, core P11-2-1).

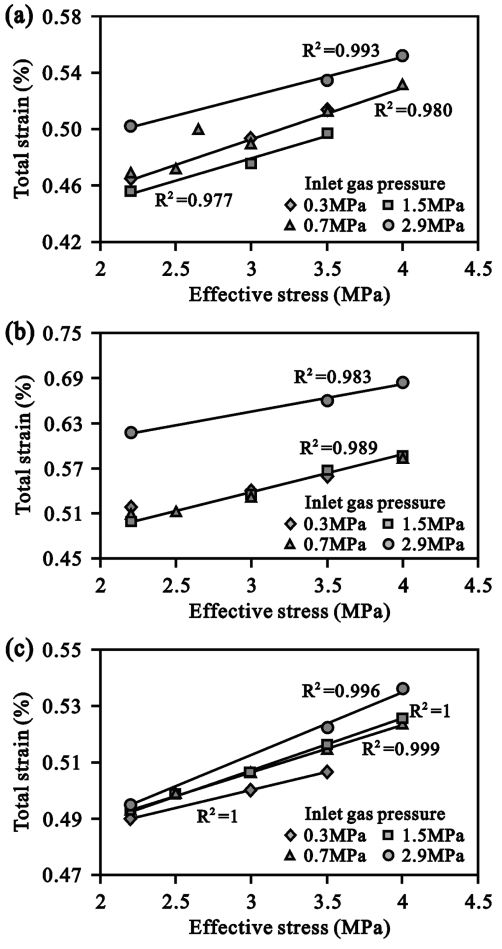

Figure 12. Relationship between the effective stress and the total strain of coal under constant gas pressure conditions (a, core D2-2; b, core S1; and c, core P11-2-1).

All of the observations above suggest the possible mechanisms of the gas permeability change for different rank coals during the pressure depletion under a constant confining stress condition, and it can be considered that the gas permeability change is comprehensively influenced by the gas slippage, the coal matrix shrinkage, and the effective stress increase. The first is related to the kinetics of the gas flow through tightly porous media and becomes significant at low pressures.[3,34] The last two will cause the deformation of the pore-fracture structure of coals, which, in turn, alters the coal permeability.[11−14]

For the three cores studied in this paper, during the pressure decline under a 4.3 MPa confining stress condition, (a) the effective stress effect was believed to be consistently negative, (b) the effect of the gas slippage on the permeability was positive and became significant as the inlet gas pressure was less than 1.5 MPa, and (c) the impact from the matrix shrinkage was a significant cause of permeability variation. For high-volatile A bituminous coal core D2-2, the negative effects from matrix shrinkage and the effective stress contributing toward the reduction in the permeability were offset by the positive effect from the gas slippage at inlet gas pressures of less than 1.5 MPa. However, with respect to medium-volatile bituminous coal core S1 and anthracite coal core P11-2-1, the positive effect from the matrix shrinkage occurred at inlet pressures of less than approximately 2.5 and 3.5 MPa, respectively. At these two stages, the summative positive effects from the matrix shrinkage and the gas slippage on the permeability become greater than the negative effect from the effective stress, causing the increase in permeability. In addition, the initial decrease in the permeability of core S1 at inlet gas pressures of greater than approximately 2.5 MPa was because the negative effect from the effective stress and the matrix shrinkage dominated at higher gas pressures.

4. CONCLUSION

(1) This study has shown that the CO_2 permeability of different rank coals varied widely during gas pressure depletion under a 4.3 MPa confining stress condition. The permeability variations are superimposed effects from the effective stress increase, the gas slippage, and the coal matrix shrinkage. (2) Effective stress increase is one of the most significant factors impacting coal permeability losses during the pressure depletion. Coal cleat compressibility reflects the sensitivity of the permeability to the effective stress. Generally, lower permeable coal with higher stress sensitivity will have a less permeability loss. (3) The positive effect from the gas slippage on the permeability can be uniformly expressed exponentially and usually became more significant at mean gas pressures of less than 0.8 MPa. The permeability increment values were low overall and varied from 0.008 to 165.374 μD as the gas pressure decreased from 4.1 to 0.5 MPa under a 4.3 MPa confining stress condition. (4) The

dx.doi.org/10.1021/ef402285n | Energy Fuels 2014, 28, 987−996

Table 3. Mathematical Expressions Obtained by Correlation Analyses for the Three Cores[a]

core number	$\Delta k_{eff}(p_t)$ (mD)	$\Delta k_{sli}(p_t)$ (mD)	$\Delta k_{shr}(p_t)$ (mD)
D2-2	$\Delta k_{eff}(p_t) = -0.0084(p_i - p_t)$	$\Delta k_{sli}(p_t) = 0.0109(p_t - p_2)^{-0.5569}$	$\Delta k_{shr}(p_t) = 0.0002(p_t - p_2)^2 + 0.015(p_t - p_2) - 0.0294$
S1	$\Delta k_{eff}(p_t) = -0.0717(p_i - p_t)$	$\Delta k_{sli}(p_t) = 0.0847(p_t - p_2)^{-0.7013}$	$\Delta k_{shr}(p_t) = 0.0522(p_t - p_2)^2 + 0.2901(p_t - p_2) - 0.2156$
P11-2-1	$\Delta k_{eff}(p_t) = -0.0309(p_i - p_t)$	$\Delta k_{sli}(p_t) = 0.0426(p_t - p_2)^{-0.5841}$	$\Delta k_{shr}(p_t) = 0.0171(p_t - p_2)^2 + 0.1208(p_t - p_2) - 0.0035$

[a] $\Delta k_{eff}(p_t)$, $\Delta k_{sli}(p_t)$, and $\Delta k_{shr}(p_t)$ are the permeability increments induced by the effective stress, the gas slippage, and the matrix shrinkage, respectively.

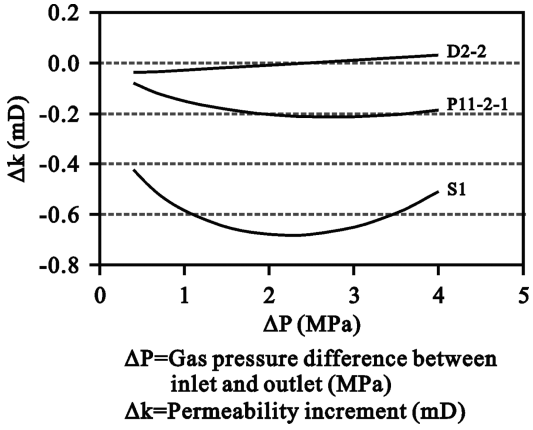

Figure 13. Ideal change tendency of the total permeability increment caused by the effective stress, the gas slippage, and the matrix shrinkage under a 4.3 MPa confining stress condition.

changes of the matrix-shrinkage-induced permeability increment varied for different rank coals, and the magnitude of the increment ranged from −694.672 to 31.651 μD. During the pressure depletion, the effect of the matrix shrinkage on the permeability was negative for high-volatile A bituminous coal, whereas with respect to medium-volatile bituminous coal and anthracite coal, the effect became positive at mean gas pressures of less than approximately 1.3 and 1.8 MPa, respectively. (5) Coal permeability variation associated with the effective stress increase and the matrix shrinkage is the result of the occurrence of strain in coals.

AUTHOR INFORMATION

Corresponding Author

*Telephone: 86-10-82320892. Fax: 86-10-82326850. E-mail: dmliu@cugb.edu.cn.

Notes

The authors declare no competing financial interest.

ACKNOWLEDGMENTS

This study was supported by the National Major Research Program for Science and Technology of China (2011ZX05034-001 and 2011ZX05062-006), the National Natural Science Foundation of China (U1262104), the Fundamental Research Funds for the Central Universities (2652013007), the Program for Excellent Doctoral Dissertation Supervision of Beijing (YB20101141501), the Program for New Century Excellent Talents in University (NCET-11-0721), and the Foundation for the Author of National Excellent Doctoral Dissertation of People's Republic of China (Grant 201253). The authors are grateful to the anonymous reviewers for their careful reviews and detailed comments.

REFERENCES

(1) Reiss, L. H. *The Reservoir Engineering Aspects of Fractured Formations*; Gulf Publishing Co.: Houston, TX, 1980; p 20.
(2) Seidle, J. P.; Jeansonne, M. W.; Erickson, D. J. Application of matchstick geometry to stress dependent permeability in coals. *Proceedings of the SPE Rocky Mountain Regional Meeting*; Casper, WY, May 18−21, 1992; SPE 24361.
(3) Harpalani, S.; Chen, G. *Geotech. Geol. Eng.* **1997**, *15*, 303−325.
(4) Cui, X.; Bustin, R. M. *AAPG Bull.* **2005**, *89*, 1181−1202.
(5) Shi, J.; Durucan, S. *Transp. Porous Med.* **2004**, *56*, 1−16.
(6) Shi, J.; Durucan, S. *SPE Reservoir Eval. Eng.* **2005**, *8*, 291−299.
(7) Liu, S.; Harpalani, S.; Pillalamarry, M. *Fuel* **2012**, *94*, 117−124.
(8) Harpalani, S.; Schraufnagel, A. *Int. J. Min. Geol. Eng.* **1990**, *8*, 369−384.
(9) Balan, H. O.; Gumrah, F. *Int. J. Coal Geol.* **2009**, *77*, 203−213.
(10) Clarkson, C. R.; Bustin, R. M. *SPE Reservoir Eval. Eng.* **2011**, *14*, 60−75.
(11) Zhang, H.; Liu, J.; Elsworth, D. *Int. J. Rock Mech. Min. Sci.* **2008**, *45*, 1226−1236.
(12) Huy, P. Q.; Sasaki, K.; Sugai, Y.; Ichikawa, S. *Int. J. Coal Geol.* **2010**, *83*, 1−10.
(13) Liu, H.; Rutqvist, J. *Transp. Porous Med.* **2010**, *82*, 157−171.
(14) Liu, J.; Chen, Z.; Elsworth, D.; Miao, X.; Mao, X. *Fuel* **2011**, *90*, 2987−2997.
(15) Levine, J. R. *Coalbed Methane and Coal Geology*; Geological Society Special Publications: London, U.K., 1996; pp 197−212.
(16) Gilman, A.; Beckie, R. *Transp. Porous Med.* **2000**, *41*, 1−16.
(17) Yang, K.; Lu, X.; Lin, Y.; Neimark, A. V. *Energy Fuels* **2010**, *24*, 5955−5964.
(18) Yang, K.; Lu, X.; Lin, Y.; Neimark, A. V. *J. Geophys. Res.* **2011**, *116*, B08212.
(19) Mitra, A.; Harpalani, S.; Liu, S. *Fuel* **2012**, *94*, 110−116.
(20) Chikatamarla, L.; Cui, X.; Bustin, R. M. Implications of volumetric swelling/shrinkage of coal in sequestration of acid gases. *Proceedings of the International Coalbed Methane Symposium*; Tuscaloosa, AL, May 3−7, 2004; Paper 0435.
(21) Sereshki, F.; Hosseini, S. A.; Aziz, N.; Porter, I. *Int. J. Eng. Sci.* **2008**, *19*, 15−22.
(22) Day, S.; Fry, R.; Sakurovs, R. *Int. J. Coal Geol.* **2008**, *74*, 41−52.
(23) Karacan, C. Ö. *Energy Fuels* **2003**, *17*, 1595−1608.
(24) Karacan, C. Ö. *Int. J. Coal Geol.* **2007**, *72*, 209−220.
(25) Larsen, J. W. *Int. J. Coal Geol.* **2004**, *57*, 63−70.
(26) Kolak, J. J.; Burruss, R. C. *Energy Fuels* **2006**, *20*, 566−574.
(27) McKee, C. R.; Bumb, A. C.; Koenig, R. A. *SPE Form. Eval.* **1988**, *3*, 81−91.
(28) Cui, X.; Bustin, R. M.; Dipple, G. *Fuel* **2004**, *83*, 293−303.
(29) Gu, F.; Chalaturnyk, R. J. *J. Can. Pet. Technol.* **2005**, *44*, 23−32.
(30) Clarkson, C. R.; Pan, Z.; Palmer, I.; Harpalani, S. *SPE J.* **2008**, *15*, 152−159.
(31) Palmer, I. *Int. J. Coal Geol.* **2009**, *77*, 119−126.
(32) Connell, L. D.; Lu, M.; Pan, Z. *Int. J. Coal Geol.* **2010**, *84*, 103−114.
(33) Harpalani, S.; Schraufnagel, A. Influence of matrix shrinkage and compressibility on gas production from coalbed methane reservoirs. *Proceedings of the SPE Annual Technical Conference and Exhibition*; New Orleans, LA, Sept 23−26, 1990; SPE 20729.
(34) Li, J.; Liu, D.; Yao, Y.; Cai, Y.; Chen, Y. *Fuel* **2013**, *111*, 606−612.

(35) Yao, Y.; Liu, D.; Tang, D.; Tang, S.; Che, Y.; Huang, W. *Int. J. Coal Geol.* **2009**, *78*, 1−15.
(36) Liu, D.; Yao, Y.; Tang, D.; Tang, S.; Che, Y.; Huang, W. *Int. J. Coal Geol.* **2009**, *79*, 97−112.
(37) Li, J.; Liu, D.; Yao, Y.; Cai, Y.; Guo, X. *Energy Explor. Exploit.* **2013**, *31*, 267−285.
(38) Li, J.; Liu, D.; Yao, Y.; Cai, Y. *Int. J. Coal Geol.* **2011**, *87*, 121−127.
(39) Somerton, W. H.; Söylemezoğlu, I. M.; Dudley, R. C. *Int. J. Rock Mech. Min. Sci.* **1975**, *12*, 129−145.
(40) Durucan, S.; Edwards, J. S. *Min. Sci. Technol.* **1986**, *3*, 205−216.
(41) Pan, Z. J.; Connell, L. D.; Camilleri, M. *Int. J. Coal Geol.* **2010**, *82*, 252−261.
(42) Zheng, G.; Pan, Z.; Chen, Z.; Tang, S.; Connell, L. D.; Zhang, S.; Wang, B. *Energy Explor. Exploit.* **2012**, *30*, 451−476.
(43) Klinkenberg, L. J. *Drilling and Production Practice*; American Petroleum Institute: Washington, D.C., 1941; pp 200−213.
(44) Wang, S.; Elsworth, D.; Liu, J. *Int. J. Coal Geol.* **2011**, *87*, 13−25.